
Investigating Distributional Robustness: Semantic Perturbations Using Generative Models

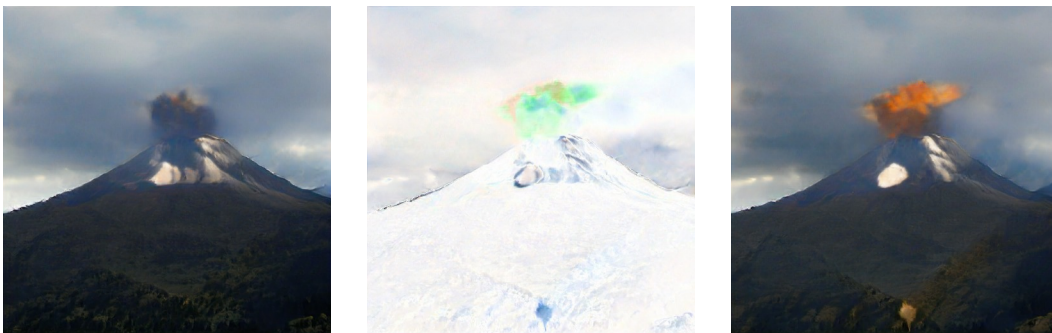
Isaac Dunn Laura Hanu Hadrien Pouget Daniel Kroening Tom Melham
Department of Computer Science, University of Oxford
isaac.dunn@cs.ox.ac.uk

Abstract

In many situations, the i.i.d. assumption cannot be relied upon; training datasets are not representative of the full range of inputs that will be encountered during deployment. Especially in safety-critical applications such as autonomous driving or medical devices, it is essential that we can trust our models to remain performant. In this paper, we introduce a new method for perturbing the semantic features of images (e.g. shape, location, texture, and colour) for the purpose of evaluating classifiers' robustness to these changes. We produce these perturbations by performing small adjustments to the latent activation values of a trained generative neural network (GAN), leveraging its ability to represent diverse semantic properties of an image. We find that state-of-the-art classifiers are not robust to subtle shifts in the semantic features of input data, and that adversarial training against pixel-space perturbations is not just unhelpful: it is *counterproductive*.

1 Introduction

Deep learning models have proven to be powerful tools for tasks including image classification [1, 2], with the ability to automatically identify useful features of their training images and combine these to provide accurate label predictions [3]. Under the assumption that data are independently and identically distributed (i.i.d.), they have shown a remarkable ability to generalise to unseen inputs [4]. However, it is increasingly clear that the performance of these models drops drastically without this assumption; optimising for i.i.d. accuracy alone results in models that are not robust to even modest distributional shifts [5–8]. This is concerning because the non-static nature of the real world may well cause the distribution of inputs to shift during deployment, and because it is difficult for any finite training set to capture



(a) Unperturbed generated image. (b) Semantic perturbation. (c) Semantically perturbed image.

Figure 1: A semantic perturbation changing the computed classification from ‘volcano’ to target label ‘goldfish’ by darkening the sky, causing an eruption of lava, slightly flattening the curve of the volcano, and adding a rocky outcrop in the foreground.

the full range of inputs that may be encountered. A model’s lack of robustness likely occurs due in part to over-reliance on non-robust features that correlate well under the i.i.d. assumption but stop providing useful information after a shift [9]. Before deploying models, especially in safety-critical contexts, we must evaluate their robustness to possible unknown shifts in the distribution of encountered inputs.

In this work, we introduce a new method that evaluates the robustness of neural networks to *semantic perturbations*: changes to a broad class of meaningful features, including the shape, location, size, pose, colour, and texture of the objects in an image. Rather than hand-coding these features, we exploit a generative neural network’s ability to learn and encode the full range of meaningful features of an image distribution [10]. By introducing perturbations to the latent activation values of layers in a trained generator network, we can cause semantic perturbations to the features of the generated images (Figure 1). Since different layers of the generator encode features at different levels of granularity, these perturbations can affect a rich set of features that vary from as coarse-grained as global semantic properties to as fine-grained as a cluster of a few pixels. Our method simply searches for such perturbations so that the perturbed generated image is mislabelled by the classifier we wish to evaluate.

We use this new method to evaluate the robustness of state-of-the-art ImageNet classifiers to subtle semantic shifts. Besides finding that these models are not robust in this sense, we find that using classifiers adversarially that were trained to be robust to bounded pixel perturbations actually *decreases* robustness to semantic perturbations. This may be because such classifiers must necessarily depend more on high-level semantic features of images than classifiers optimised for accuracy on i.i.d. inputs, which tend to rely on low-level features such as texture [11]. Our results strengthen and expand upon related findings from Yin et al. [12], who find that classifiers robust to pixel-level perturbations are less robust to corruptions of certain hand-selected features such as artificial ‘fog’ and 2D sinusoids.

2 Background

Robustness under distributional shift When training a discriminative neural network, the goal is typically to minimise the expected loss $\mathbb{E}_{(x,y) \sim P_0} [\ell(x,y;\theta)]$ with respect to the model parameters θ , where P_0 is the training distribution over feature space \mathbb{X} and labels in \mathbb{Y} . In real-world scenarios, however, we cannot depend on the distribution at deployment remaining identical to P_0 (i.e. we cannot rely on the i.i.d. assumption). To ensure that models behave well in practice, it is necessary to make distributionally robust models: they should perform well even after a shift to their input distribution. Studies have shown that there are many possible shifts to which classifiers are not robust, motivating a large body of literature which deals with identifying and correcting these problems [5–8, 13–15].

Generative Adversarial Networks GANs are an approach to training generative neural networks that map from a known standard probability distribution to the distribution of the training data. See a tutorial for details [16]. While other types of generative networks exist, we focus on the use of GANs in this work for their crispness. Generative networks have been found to display an interesting property: different layers, and even different neurons, encode different kinds of features of the image. Earlier layers tend to encode higher-level information about objects in the image, whereas later layers deal more with “low-level materials, edges, and colours” [10, p.7]. In addition, it is possible to vary features such as zoom, object position and rotation, simply by moving the input to the model in a linear walk [17].

3 Related Work

Measuring distributional robustness This paper builds on a body of work examining trained models’ robustness to distributional shifts. One approach is to apply a hand-selected range of possible corruptions such as Gaussian noise or simulated effects such as fog or motion blur. Such robustness benchmarks have been created for datasets including traffic signs [18], ImageNet [8], MNIST [19] and Cityscapes [20]. Snoek et al. [21] evaluate the robustness of the calibration of classifiers’ *confidences* to rotated and translated images, as well as to out-of-distribution inputs such as not-MNIST [22]. Another approach is to gather new data, either replicating original dataset creation processes [23] or deliberately gathering data representing a challenging shift in distribution [24]; in both cases, classifiers were found to fail to generalise to the new distributions. Our paper builds on the foundations laid by these works, providing automaticity by evaluating robustness to *learnt* features.

Adversarial robustness There has been much recent work on ‘adversarial examples’: inputs deliberately crafted by an adversary to fool a model [25]. In this literature, an attacker is modelled as having certain capabilities to construct pathological inputs, while the ‘defender’ aims to create systems that are robustly correct to all inputs within this threat model. Such attacks can be viewed as the worst-case distributional shift within the threat model. The customary threat model is constrained perturbations to the pixel values of a given image [26], for which adversarial robustness does not imply robustness to semantic changes that induce large changes in pixel values. But there is a burgeoning interest in new threat models that allow *meaningful* changes to given images. While the purpose of our method is to evaluate models’ distributional robustness to plausible semantic shifts, rather than to serve as an adversarial attack—it is unclear that an attacker could present a perturbed image to a deployed model without write access to the model’s inputs—some existing semantic ‘attacks’ are related to our method.

Semantic adversarial robustness Initially, semantic adversarial examples were constructed using hand-coded methods that perturbed features such as colouring [27], rotations and translations [28], and corruptions such as blurring and fog [29] in an ad-hoc manner. Another possible approach, albeit prohibitively expensive for most domains, is to write an invertible differentiable renderer and perturb its parameters to effect semantic changes in the scene [30, 31]. More recently, methods have been proposed that use generative models to avoid the need to hand-code specific features to perturb.

Qiu et al. [32] use a dataset labelled with various semantic features to train a generative model that allows inputs determining these features to be adversarially adjusted. Bhattad et al. [33] utilise learnt colourisation and texture-transfer models to identify worst-case changes to the colour and texture of given images. Gowal et al. [34] adversarially compose disentangled learned representations of different inputs. Dunn et al. [35] train a GAN to output a distribution of images that fools the target classifier. Three imaginative papers construct semantic adversarial examples using some search procedure to identify a suitable input to a trained generative model [36–38]. We build on the common theme: using a generative model to learn semantic features, avoiding the need to select and code these by hand. However, our method is the first to perturb the generator network’s latent activations—not just the input. This leverages the *full* range of feature representations learnt from the training dataset, rather than just the global semantics encoded in the input, allowing for a much richer space of manipulations.

4 Computing semantic perturbations using generative models

Suppose that we have a trained, differentiable image classifier $f : \mathbb{X} \rightarrow \mathbb{R}^{|\mathbb{Y}|}$ whose robustness we would like to test, where $\mathbb{X} = \mathbb{R}^{3 \times w \times h}$ is RGB pixel space and \mathbb{Y} is the set of class labels over which f outputs a confidence distribution. Suppose that we also have a trained generator neural network $g : \mathbb{Z} \rightarrow \mathbb{X}$, which maps from a standard Gaussian distribution over its input space $\mathbb{Z} = \mathbb{R}^m$ to the distribution of training images. Although we use the generator of a GAN pair, any generative model would be equally suitable.

Since a feedforward network is a sequence of layers, we can consider g to be a composition of functions $g = g_n \circ g_{n-1} \circ \dots \circ g_1$. For instance, in our experiments, we decompose BigGAN [39] into its residual blocks. Here, $g_i : \mathbb{A}_{i-1} \rightarrow \mathbb{A}_i$ is the i th layer, taking activations $a_{i-1} \in \mathbb{A}_{i-1}$ from the previous layer and outputting the resulting activation tensor $g_i(a_{i-1}) \in \mathbb{A}_i$. Splitting in this way allow us to introduce a perturbation $p_i \in \mathbb{A}_i$ to layer i ’s activations, before continuing the forward pass through the rest of the generator. Given such a perturbation tensor $p_i \in \mathbb{A}_i$ for each layer i , we can define perturbed layer functions $g'_i(a_{i-1}) = g_i(a_{i-1}) + p_i$. By performing such perturbations at every activation space, we obtain the semantically-perturbed output of the entire generator, $g'(z; p_0, \dots, p_n) = (g'_n \circ g'_{n-1} \circ \dots \circ g'_1)(z + p_0)$.

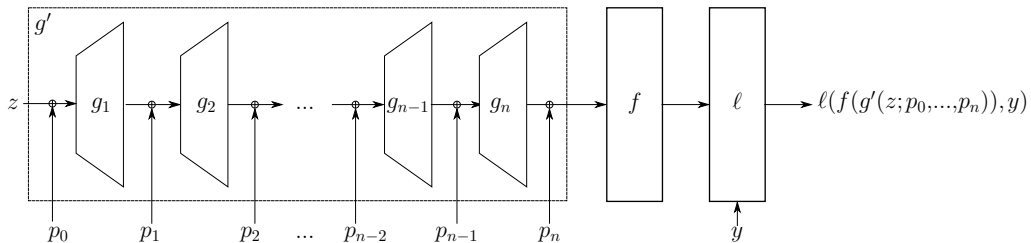


Figure 2: Illustration of a forward pass with semantic perturbations to the latent activation values.

Suppose that we have sampled some generator input z , and automatically determined the correct label y of its image under the generator when unperturbed, $g'(z; 0, \dots, 0)$. This is best done using a conditional generator that also takes a label as input [40], but can also be achieved by assuming that the classifier’s initial output is correct. We now need a procedure to identify suitable perturbation tensors $\mathbf{p}^* = (p_0^*, \dots, p_n^*) \in \mathbb{A}_0 \times \dots \times \mathbb{A}_n$ such that the classifier’s output on $g'(z; \mathbf{p}^*)$ is not y but some other label, while the true label of $g'(z; \mathbf{p}^*)$ remains y .

Ensuring misclassification We can define a loss function $\ell: \mathbb{R}^{|\mathbb{Y}|} \times \mathbb{Y} \rightarrow \mathbb{R}$ such that $\ell(f(g'(z; \mathbf{p})), y)$ is minimised when the classifier predicts any label but the correct y , or such that $\ell(f(g'(z; \mathbf{p})), t)$ is minimised when the classifier incorrectly predicts target label t . There are many possibilities, but in this paper we focus on the latter case only, using $\ell(f(x), t) = \max_{j \in \mathbb{Y}} f(x)_j - f(x)_t$, the variant found to be most effective by Carlini and Wagner [41]. Noting that ℓ , f and each g'_i are differentiable, we use the usual backpropagation algorithm to compute the derivative of $\ell(f(g'(z; \mathbf{p})), y)$ with respect to \mathbf{p} . We then use a gradient-descent optimisation over \mathbf{p} to find a perturbation \mathbf{p}^* that minimises ℓ . By definition of ℓ , this optimal \mathbf{p}^* will ensure that the classifier mislabels perturbed image $g'(z; \mathbf{p}^*)$.

Ensuring the true label remains unchanged But we also need the true label of $g'(z; \mathbf{p}^*)$ to remain y , else f might in fact be predicting the correct label. Our approach is to assume that *small* semantic changes to an image will not change its correct label (and we verify this in our experiments). So we would ideally like to identify the smallest perturbation that induces the kind of mislabelling we are investigating. The approach we take is to constrain the maximum magnitude of the perturbation—computed as the Euclidean norm of the vector obtained by ‘flattening’ and concatenating the perturbation tensors p_i —and gradually relaxing this constraint during optimisation until a perturbation \mathbf{p}^* inducing the desired mislabelling is found. The quicker the constraint is relaxed, the quicker a mislabelling is found, but the larger the expected perturbation.

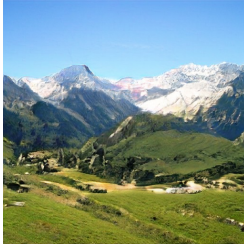
Per-neuron perturbation scaling to promote uniformity The typical activation values of separate neurons differ in scale, even within a single layer. If one varies from -1 to 1 , while another varies from -0.1 to 0.1 , then a perturbation of magnitude 0.5 is likely to have quite different downstream effects on the image depending on which of these neurons it affects. To correct for this, we scale the perturbation for each neuron to the empirically-measured range. That is, rather than adding perturbation tensor p_i directly to the activation tensor at layer i , we add $p_i \odot \sigma_i$, where \odot is element-wise multiplication and σ_i is an empirically-measured tensor of standard deviations of the activation values at layer i .

Even with this scaling, it appears that perturbations can have quite different human-perceived ‘magnitudes’ of downstream effect on the image, depending on which neurons are perturbed. In the present work, this did not pose a significant problem, since state-of-the-art classifiers require only small perturbations before their lack of robustness is revealed. But as classifiers improve, it will become increasingly important that perturbations of similar magnitude have similar downstream visual effect sizes. This can be obtained by optimising hyperparameters that scale the perturbation to each neuron as σ does above. For now, our codebase implements this at a per-layer level, since early layers tend to have larger influence on the final image, changing objects and settings, while later layers have subtler effects. In this paper each weight is always either 1 or 0 .

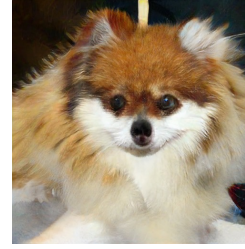
5 Experimental Evaluation

In this section, we apply our method to evaluate the robustness of state-of-the-art classifiers to semantic perturbations, primarily in the context of ImageNet-1K classification [42], perturbing the semantic features learnt by a pre-trained BigGAN [39]. We evaluate normally-trained classifiers, and two ‘robust’ classifiers adversarially trained against bounded pixel-space perturbations. First, the state-of-the-art on ImageNet, EfficientNet-B4 with NoisyStudent training [2]. This was the highest-accuracy classifier for which pre-trained weights were available. Next, the standard ResNet50 classifier [43]. Finally, two ResNet50 classifiers adversarially trained against pixel-space perturbations: one from Engstrom et al. [44] trained using an l_2 -norm PGD attack with radius $\epsilon = 0.3$, and another from Wong et al. [45], trained with the FGSM attack for robustness against l_∞ with $\epsilon = 4/255$. See Appendix A for further details.

We focus exclusively on the most concerning case: targeted misclassifications, for which a randomly pre-determined target label $t \in \mathbb{Y}$ is chosen for each semantic perturbation. We can quantitatively assess the robustness of a classifier by measuring how often we can find such misclassification-inducing perturba-



(a) Perturbed from '*alp*' (left) to '*bison*' (right) by adjusting the shapes of the mountains, ironing out rugged details and introducing shadowy boulders.



(b) Perturbed from '*Pomeranian (dog breed)*' (left) to '*American lobster*' (right) by changing the fur colour and dulling glints in the eyes and nose.



(c) Perturbed from '*sea snake*' to '*crossword*' by repositioning the snake and increasing the roughness of the sea floor.



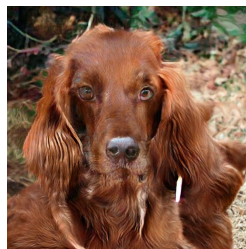
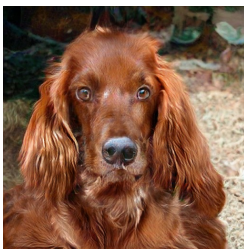
(d) Perturbed from '*robin*' to '*keyboard*' by quantising the foreground and background undergrowth in more regular patterns of light and dark.



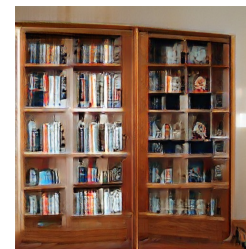
(e) Perturbed from '*backpack*' to '*remote control*' by recolouring the button and seam, and reshaping the outline.



(f) Perturbed from '*mountain tent*' to '*Norwich terrier*' by flattening the mountain range and adding a suspiciously dog-shaped rock formation.



(g) Perturbed from '*Irish setter*' to '*tusker*' (elephant) by adding background undergrowth, raising the ears, shrinking the nose and extending the body.



(h) Perturbed from '*bookcase*' to '*consommé*' (soup) by replacing the contents of some shelves and thickening the wooden frame.

Figure 3: A selection of examples to demonstrate a range of possible semantic perturbations. See Appendix C.2 for further examples.

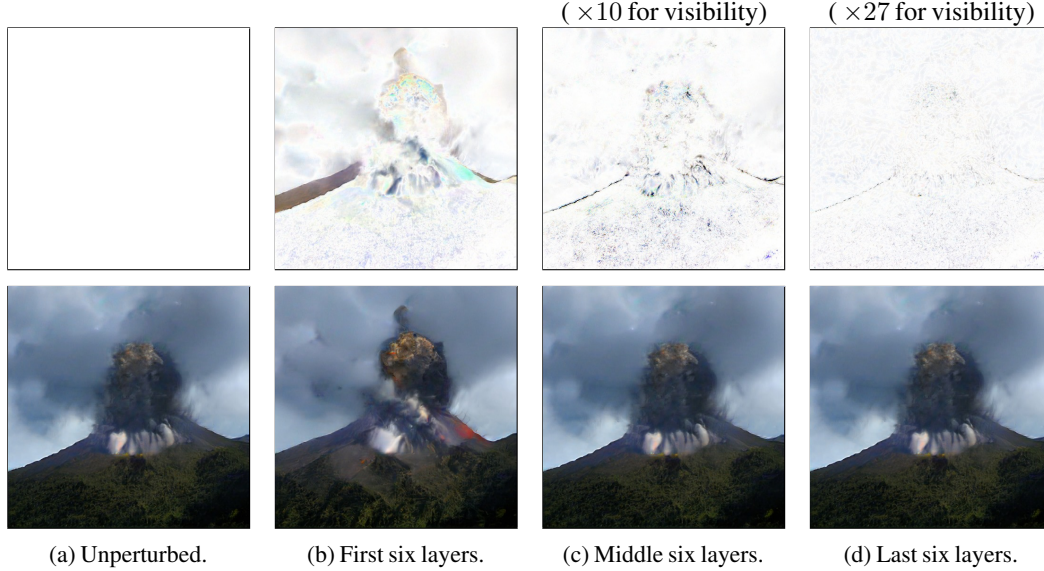


Figure 4: The effect of perturbing activations at different layers in the generator, as indicated in the captions. Differences with the unperturbed image are shown above each perturbed image. The perturbed images are classified as goldfish. Note the decreasing granularity of changes.

tions given a maximum allowable perturbation size. To do this, we sample inputs to the generator, identify suitable semantic perturbations, and measure their magnitudes—recall that we relax the constraint on the perturbation magnitude until the desired misclassification is induced. To evaluate robustness to changes to different feature granularities, we repeat this robustness analysis, but restrict the perturbations to affect different subsets of layers. For full details of our experiments, refer to Appendix B.

We also run our experiments on the much simpler (and correspondingly easier to robustly classify) MNIST dataset [46], using two classifiers: one optimised for i.i.d. accuracy, and one adversarially trained to be robust to an l_2 -norm projected gradient descent attack with $\epsilon = 0.3$. We provide some discussion in Section 5.2, and results are available in Appendix D.

5.1 Results

Table 1 reports the average magnitude of the misclassification-inducing semantic perturbations, allowing for easy comparison between classifiers for different perturbation types. Figure 5 elaborates on this, plotting the relationships between perturbation magnitude and the proportion of inputs for which this magnitude is sufficient to cause the classifier to predict the target label. These results exclude the unperturbed generated images of label y for which the classifier already predicts a label other than y , and those judged by a human not to be of label y . They also exclude perturbed images for which y is no longer judged to be the true class. See Appendix B.2 for full details of our procedure.

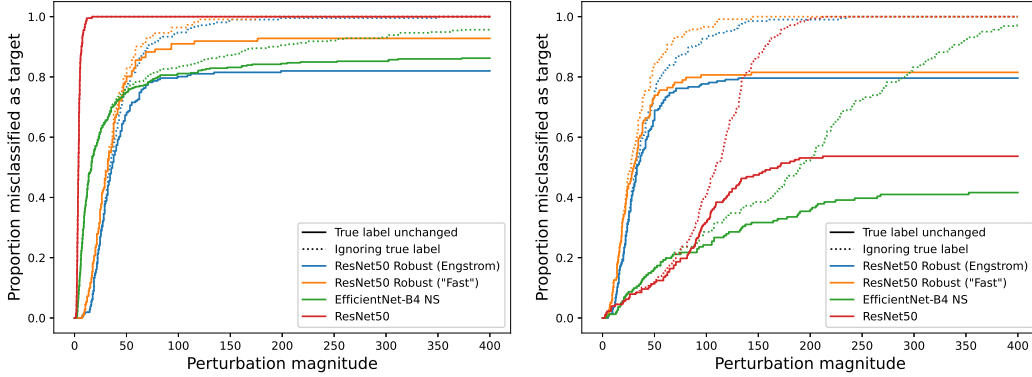
5.2 Discussion

Qualitative results The results in Figure 3 and Appendix C.2 demonstrate that perturbing the latent activations of generative networks has diverse and meaningful effects. The examples in Figure 4 and Appendix C.1 demonstrate that the perturbing the activations at different layers make changes of different granularity: perturbations to layers early in the generator tend to affect high-level properties such as object shape, while perturbations to later layers adjust finer-grained features such as texture. The wide range of semantic changes automatically generated by our method helps create a more complete evaluation of a classifier’s robustness.

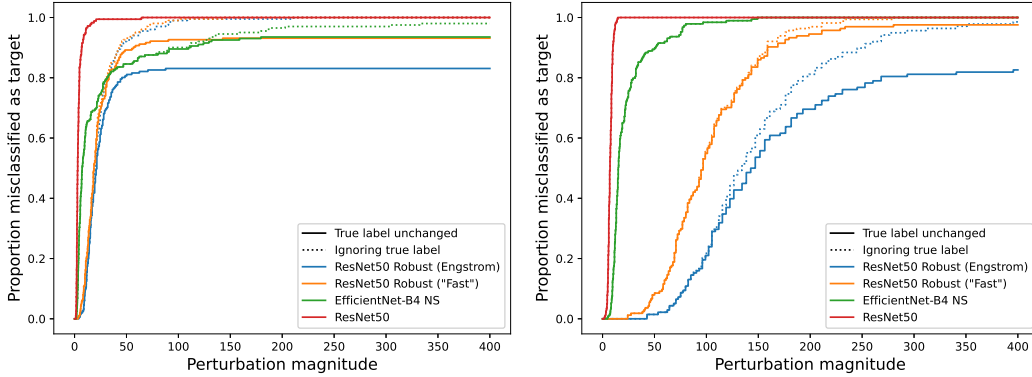
None of the classifiers are robust to semantic perturbations Figure 5a shows that for all four classifiers, our method finds misclassification-inducing perturbations for over 80% of the initial generated images, even with relatively small perturbation magnitudes. This result is consistent with

Table 1: Mean magnitudes of misclassification-inducing perturbations. Headers indicate the layers in the generator at which activations are perturbed. Compare results within each column.

	All layers	First six only	Middle six only	Last six only
Robust (Engstrom) [44]	36	33	21	141
Robust (“Fast”) [45]	35	29	22	102
EfficientNet [2]	36	97	22	24
ResNet50 [43]	4.2	89	4.2	7.4



(a) Activation values perturbed at all BigGAN layers. (b) Activation values perturbed in the first six layers only.



(c) Activations perturbed in the middle six layers only. (d) Activation values perturbed in the last six layers only.

Figure 5: Graphs showing how the proportion of perturbations that induce the targeted misclassification increases with perturbation magnitude. Results are shown for four classifiers: two adversarially-trained classifiers (Engstrom et al. [44] and “Fast” [45]), EfficientNet-B4 NS [2], and standard ResNet50 [43]. The solid lines exclude the perturbed images for which a human judges that the perturbation does not change the true label of the image; the dotted lines, for reference, include these.

the notion that trained classifiers have learnt to rely on spurious (or at least fragile) feature correlations that may not generalise beyond the training regime. For instance, relying on background colour to identify the foreground object may work well if this correlation holds—as it would both during normal i.i.d. training and adversarial training—but this should not be relied upon at deployment.

Pixel-space robustness improves robustness to some semantic perturbations The lower average magnitudes required for the pixel-robust classifiers when perturbing the final six layers, as seen in the last column of Table 1 and the correspondingly flatter curves in Figure 5d, demonstrate that adversarial training generalises somewhat to confer robustness to fine-grained semantic perturbations. The slightly gentler gradient at the beginning of Figure 5c suggests that this even provides some limited robustness to

small semantic perturbations of medium granularity. In both cases, this may be because the perturbations fall within or nearby the pixel-space L_p -norm ball that the classifier is trained to be robust within.

But robustness to pixel-space perturbations is a double-edged sword Perturbations to activations in the early layers of a generator induce changes to high-level semantic properties of an image. These have a large magnitude when measured in pixel space, so it is unsurprising that classifiers trained to be robust to norm-constrained pixel perturbations do not have improved robustness to such semantic perturbations. More surprisingly, Figure 5b and Table 1 show that pixel-space robustness in fact considerably *worsens* robustness to semantic perturbations to the high-level features encoded in the first six generator layers. This may be because non-robust classifiers ordinarily depend mainly on low-level features such as texture [11]. Conversely, pixel-space robust classifiers have been trained to ignore these low-level features, and so depend instead on high-level features. However, they are still free to rely on fragile correlations in the high-level features, and so their robustness to high-level semantic perturbations is decreased.

There is already some evidence that classifiers optimised for robustness to constrained adversarial pixel perturbations seem to have decreased robustness to corruptions concentrated in the low-frequency Fourier domain [12], decreased robustness to invariance-based attacks that change the true label but maintain the model’s prediction [47] and little robustness to various hand-coded corruptions not encountered at training time [48]. Our finding that such models also have significantly decreased robustness to high-level semantic feature perturbations strengthens and generalises these results.

MNIST The simplicity of the MNIST classification task suggests that constructing a robust classifier for MNIST should be significantly easier than for ImageNet. We find that adversarial training against pixel perturbations does not improve robustness to coarse-grained semantic perturbations on MNIST, but neither does it worsen it. This is likely because the simplicity and low resolution of the dataset means that there is much less of a difference between pixel-space perturbations and semantic perturbations, relative to ImageNet. See Appendix D for results and discussion.

5.3 Threats to validity

Our findings depend on consistent and reasonable judgements of image class. To prevent confirmation bias from distorting the results, we used a labeller who was blind to the purpose of their judgements. To eliminate potential between-person differences, we used the same labeller throughout. We designed the labelling interface to be unambiguous (see Appendix B.2 for a screenshot). Lastly, we verified that a sample of the labels judgements were reasonable, and provide them in Appendix C.2.

A threat to external validity is that our findings fail to generalise to other classifiers, training procedures, or domains. We note that if true, this would in itself be a surprising result worthy of investigation.

6 Conclusion

Since the i.i.d. assumption cannot be relied upon during deployment, it is necessary for our models to remain performant when given inputs *semantically similar* to those in its training distribution. In this paper, we have introduced a new method that evaluates robustness of image classifiers to such semantic changes. In particular, by dynamically perturbing the activation values of a trained generative neural network, our method leverages its full range of learnt feature representations. This allows evaluation of robustness to features varying from high-level semantic properties such as shape and colour (encoded in earlier layers) to fine-grained features and textures (encoded in later layers).

We find that modern state-of-the-art ImageNet classifiers are not robust to semantic perturbations. Furthermore, while classifiers optimised for robustness to bounded pixel perturbations are indeed more robust to fine-grained features perturbations, this is to the detriment of their robustness to high-level perturbations. If we are to deploy trained models in the real world, we must be confident in our ability to verify their robustness to all kinds of potential distributional shifts—including to those beyond subtle semantic changes. Besides the obvious need for more robust models, our findings motivate the need for more comprehensive ways of testing classifiers, especially on meaningful distributional shifts, which are more difficult to systematically produce. Our method points to a promising direction for creating such tests, by leveraging the latent learnt representations of generative models.

Broader Impact

We believe this research can be used to make necessary-but-not-sufficient robustness tests for computer vision systems which we want to deploy in real-world situations. For example, a clinical decision support system should not fail to detect a brain tumour due to a small variation in the input data (e.g. an artefact caused by a scanner, or a change in the distribution of patients).

Regulators may therefore choose to utilise methods deriving from our work to identify flaws in safety cases for new systems—identifying these flaws before approval and deployment could prevent serious harms. Having adequate tools for this scrutiny may be particularly important given commercial incentives to deploy quickly, potentially causing developers to give inadequate consideration to safety. But care must be taken not to naïvely rely on tools based directly on our work as sufficient evidence of robustness: our method evaluates only subtle semantic shifts, which may not be the only kind of input encountered during deployment. Our method should be combined with other checks to allow for a complete evaluation of a classifier’s robustness, and indeed other properties such as bias, privacy, or fairness. These should be separately evaluated in whichever ways are appropriate for the task at hand, before a system is deemed ready for deployment.

Developers of safety-critical systems may also use tools maturing from our work to identify and rectify concerns in a system under development. By evaluating robustness to a wide range of possible semantic changes, our method can help to characterise weaknesses and therefore inform what kind of improvements need to be made to a system including a trained component. This might help bring a product safely to market more quickly than would otherwise have been possible; there is no doubt that deep learning could provide significant benefits to the safety-critical industries, once the robustness problem is solved. But equally, there are potential harms associated with speedier deployment of perfectly safe systems: safe truly autonomous vehicles could lead to mass unemployment; more generally, wide deployment of autonomous systems is likely to have unforeseen consequences.

Aside from application of developments of our method to evaluate robustness for safety, our method contributes to our gradually growing understanding of the robustness characteristics of neural networks. By strengthening the result that adversarial training against pixel perturbations may in fact be counterproductive when it comes to real-world robustness, we hope that there will be more research in the future aiming to characterise and address the robustness problem in its broadest sense. A more thorough understanding of our strengths and limitations seems essential if we are to fully reap the benefits and mitigate the risks of this still-new technology.

References

- [1] Hugo Touvron, Andrea Vedaldi, Matthijs Douze, and Hervé Jégou. Fixing the train-test resolution discrepancy: Fixefficientnet. *CoRR*, abs/2003.08237, 2020. URL <https://arxiv.org/abs/2003.08237>.
- [2] Qizhe Xie, Eduard H. Hovy, Minh-Thang Luong, and Quoc V. Le. Self-training with Noisy Student improves ImageNet classification. *CoRR*, abs/1911.04252, 2019. URL <http://arxiv.org/abs/1911.04252>.
- [3] Chris Olah, Nick Cammarata, Ludwig Schubert, Gabriel Goh, Michael Petrov, and Shan Carter. Zoom in: An introduction to circuits. *Distill*, 2020. doi: 10.23915/distill.00024.001. <https://distill.pub/2020/circuits/zoom-in>.
- [4] Behnam Neyshabur, Srinadh Bhojanapalli, David McAllester, and Nati Srebro. Exploring generalization in deep learning. In Isabelle Guyon, Ulrike von Luxburg, Samy Bengio, Hanna M. Wallach, Rob Fergus, S. V. N. Vishwanathan, and Roman Garnett, editors, *Advances in Neural Information Processing Systems 30: Annual Conference on Neural Information Processing Systems 2017, 4-9 December 2017, Long Beach, CA, USA*, pages 5947–5956, 2017. URL <http://papers.nips.cc/paper/7176-exploring-generalization-in-deep-learning>.
- [5] Amir Rosenfeld, Richard S. Zemel, and John K. Tsotsos. The elephant in the room. *CoRR*, abs/1808.03305, 2018. URL <http://arxiv.org/abs/1808.03305>.
- [6] Jason Jo and Yoshua Bengio. Measuring the tendency of CNNs to learn surface statistical regularities. *CoRR*, abs/1711.11561, 2017. URL <http://arxiv.org/abs/1711.11561>.

- [7] Robert Geirhos, Carlos R. Medina Temme, Jonas Rauber, Heiko H. Schütt, Matthias Bethge, and Felix A. Wichmann. Generalisation in humans and deep neural networks. In Samy Bengio, Hanna M. Wallach, Hugo Larochelle, Kristen Grauman, Nicolò Cesa-Bianchi, and Roman Garnett, editors, *Advances in Neural Information Processing Systems 31: Annual Conference on Neural Information Processing Systems 2018, NeurIPS 2018, 3-8 December 2018, Montréal, Canada*, pages 7549–7561, 2018. URL <http://papers.nips.cc/paper/7982-generalisation-in-humans-and-deep-neural-networks>.
- [8] Dan Hendrycks and Thomas G. Dietterich. Benchmarking neural network robustness to common corruptions and perturbations. In *7th International Conference on Learning Representations, ICLR 2019, New Orleans, LA, USA, May 6-9, 2019*. OpenReview.net, 2019. URL <https://openreview.net/forum?id=HJz6tiCqYm>.
- [9] Andrew Ilyas, Shibani Santurkar, Dimitris Tsipras, Logan Engstrom, Brandon Tran, and Aleksander Madry. Adversarial examples are not bugs, they are features. In Hanna M. Wallach, Hugo Larochelle, Alina Beygelzimer, Florence d’Alché-Buc, Emily B. Fox, and Roman Garnett, editors, *Advances in Neural Information Processing Systems 32: Annual Conference on Neural Information Processing Systems 2019, NeurIPS 2019, 8-14 December 2019, Vancouver, BC, Canada*, pages 125–136, 2019. URL <http://papers.nips.cc/paper/8307-adversarial-examples-are-not-bugs-they-are-features>.
- [10] David Bau, Jun-Yan Zhu, Hendrik Strobelt, Bolei Zhou, Joshua B. Tenenbaum, William T. Freeman, and Antonio Torralba. GAN Dissection: Visualizing and Understanding Generative Adversarial Networks. In *7th International Conference on Learning Representations, ICLR 2019, New Orleans, LA, USA, May 6-9, 2019*. OpenReview.net, 2019. URL https://openreview.net/forum?id=Hyg_X2C5FX.
- [11] Robert Geirhos, Patricia Rubisch, Claudio Michaelis, Matthias Bethge, Felix A. Wichmann, and Wieland Brendel. ImageNet-trained CNNs are biased towards texture; increasing shape bias improves accuracy and robustness. In *7th International Conference on Learning Representations, ICLR 2019, New Orleans, LA, USA, May 6-9, 2019*. OpenReview.net, 2019. URL <https://openreview.net/forum?id=Bygh9j09KX>.
- [12] Dong Yin, Raphael Gontijo Lopes, Jon Shlens, Ekin Dogus Cubuk, and Justin Gilmer. A Fourier perspective on model robustness in computer vision. In Hanna M. Wallach, Hugo Larochelle, Alina Beygelzimer, Florence d’Alché-Buc, Emily B. Fox, and Roman Garnett, editors, *Advances in Neural Information Processing Systems 32: Annual Conference on Neural Information Processing Systems 2019, NeurIPS 2019, 8-14 December 2019, Vancouver, BC, Canada*, pages 13255–13265, 2019. URL <http://papers.nips.cc/paper/9483-a-fourier-perspective-on-model-robustness-in-computer-vision>.
- [13] Dario Amodei, Chris Olah, Jacob Steinhardt, Paul F. Christiano, John Schulman, and Dan Mané. Concrete problems in AI safety. *CoRR*, abs/1606.06565, 2016. URL <http://arxiv.org/abs/1606.06565>.
- [14] Aman Sinha, Hongseok Namkoong, and John C. Duchi. Certifying some distributional robustness with principled adversarial training. In *6th International Conference on Learning Representations, ICLR 2018, Vancouver, BC, Canada, April 30 - May 3, 2018, Conference Track Proceedings*. OpenReview.net, 2018. URL <https://openreview.net/forum?id=Hk6kPgZA->.
- [15] Yue He, Zheyang Shen, and Peng Cui. NICO: A dataset towards non-i.i.d. image classification. *CoRR*, abs/1906.02899, 2019. URL <http://arxiv.org/abs/1906.02899>.
- [16] Ian J Goodfellow. NIPS 2016 Tutorial: Generative Adversarial Networks. *CoRR*, abs/1701.0, 2017. URL <http://arxiv.org/abs/1701.00160>.
- [17] Ali Jahanian, Lucy Chai, and Phillip Isola. On the "steerability" of generative adversarial networks. *CoRR*, abs/1907.07171, 2019. URL <http://arxiv.org/abs/1907.07171>.
- [18] Dogancan Temel, Gukyeon Kwon, Mohit Prabhushankar, and Ghassan AlRegib. CURE-TSR: Challenging Unreal and Real Environments for Traffic Sign Recognition. *CoRR*, abs/1712.02463, 2017. URL <http://arxiv.org/abs/1712.02463>.

- [19] Norman Mu and Justin Gilmer. MNIST-C: A robustness benchmark for computer vision. *CoRR*, abs/1906.02337, 2019. URL <http://arxiv.org/abs/1906.02337>.
- [20] Claudio Michaelis, Benjamin Mitzkus, Robert Geirhos, Evgenia Rusak, Oliver Bringmann, Alexander S. Ecker, Matthias Bethge, and Wieland Brendel. Benchmarking Robustness in Object Detection: Autonomous Driving when Winter is Coming. *CoRR*, abs/1907.07484, 2019. URL <http://arxiv.org/abs/1907.07484>.
- [21] Jasper Snoek, Yaniv Ovadia, Emily Fertig, Balaji Lakshminarayanan, Sebastian Nowozin, D. Sculley, Joshua V. Dillon, Jie Ren, and Zachary Nado. Can you trust your model’s uncertainty? Evaluating predictive uncertainty under dataset shift. In Hanna M. Wallach, Hugo Larochelle, Alina Beygelzimer, Florence d’Alché-Buc, Emily B. Fox, and Roman Garnett, editors, *Advances in Neural Information Processing Systems 32: Annual Conference on Neural Information Processing Systems 2019, NeurIPS 2019, 8-14 December 2019, Vancouver, BC, Canada*, pages 13969–13980, 2019. URL <http://papers.nips.cc/paper/9547-can-you-trust-your-models-uncertainty-evaluating-predictive-uncertainty-under-dataset-shift>.
- [22] Yaroslav Bulatov. Machine Learning, etc: notMNIST dataset, September 2011. URL <http://yaroslavvb.blogspot.com/2011/09/notmnist-dataset.html>.
- [23] Benjamin Recht, Rebecca Roelofs, Ludwig Schmidt, and Vaishal Shankar. Do ImageNet classifiers generalize to ImageNet? In Kamalika Chaudhuri and Ruslan Salakhutdinov, editors, *Proceedings of the 36th International Conference on Machine Learning, ICML 2019, 9-15 June 2019, Long Beach, California, USA*, volume 97 of *Proceedings of Machine Learning Research*, pages 5389–5400. PMLR, 2019. URL <http://proceedings.mlr.press/v97/recht19a.html>.
- [24] Dan Hendrycks, Kevin Zhao, Steven Basart, Jacob Steinhardt, and Dawn Song. Natural adversarial examples. *CoRR*, abs/1907.07174, 2019. URL <http://arxiv.org/abs/1907.07174>.
- [25] Justin Gilmer, Ryan P Adams, Ian J Goodfellow, David Andersen, and George E Dahl. Motivating the Rules of the Game for Adversarial Example Research. *CoRR*, abs/1807.0, 2018. URL <http://arxiv.org/abs/1807.06732>.
- [26] Ian J. Goodfellow, Jonathon Shlens, and Christian Szegedy. Explaining and harnessing adversarial examples. In Yoshua Bengio and Yann LeCun, editors, *3rd International Conference on Learning Representations, ICLR 2015, San Diego, CA, USA, May 7-9, 2015, Conference Track Proceedings*, 2015. URL <http://arxiv.org/abs/1412.6572>.
- [27] Hossein Hosseini and Radha Poovendran. Semantic Adversarial Examples. In *2018 IEEE Conference on Computer Vision and Pattern Recognition Workshops, CVPR Workshops 2018, Salt Lake City, UT, USA, June 18-22, 2018*, pages 1614–1619. IEEE Computer Society, 2018. doi: 10.1109/CVPRW.2018.00212. URL http://openaccess.thecvf.com/content_cvpr_2018_workshops/w32/html/Hosseini_Semantic_Adversarial_Examples_CVPR_2018_paper.html.
- [28] Logan Engstrom, Brandon Tran, Dimitris Tsipras, Ludwig Schmidt, and Aleksander Madry. Exploring the Landscape of Spatial Robustness. In Kamalika Chaudhuri and Ruslan Salakhutdinov, editors, *Proceedings of the 36th International Conference on Machine Learning, ICML 2019, 9-15 June 2019, Long Beach, California, USA*, volume 97 of *Proceedings of Machine Learning Research*, pages 1802–1811. PMLR, 2019. URL <http://proceedings.mlr.press/v97/engstrom19a.html>.
- [29] Dan Hendrycks and Thomas Dietterich. Benchmarking Neural Network Robustness to Common Corruptions and Perturbations. *arXiv:1903.12261 [cs, stat]*, March 2019. URL <http://arxiv.org/abs/1903.12261>.
- [30] Hsueh-Ti Derek Liu, Michael Tao, Chun-Liang Li, Derek Nowrouzezahrai, and Alec Jacobson. Beyond pixel norm-balls: Parametric adversaries using an analytically differentiable renderer. In *7th International Conference on Learning Representations, ICLR 2019, New Orleans, LA, USA, May 6-9, 2019*. OpenReview.net, 2019. URL <https://openreview.net/forum?id=SJl2niR9KQ>.

- [31] Lakshya Jain, Wilson Wu, Steven Chen, Uyeong Jang, Varun Chandrasekaran, Sanjit A. Seshia, and Somesh Jha. Generating semantic adversarial examples with differentiable rendering. *CoRR*, abs/1910.00727, 2019. URL <http://arxiv.org/abs/1910.00727>.
- [32] Haonan Qiu, Chaowei Xiao, Lei Yang, Xinchun Yan, Honglak Lee, and Bo Li. SemanticAdv: Generating Adversarial Examples via Attribute-conditional Image Editing. *arXiv:1906.07927 [cs, eess]*, June 2019. URL <http://arxiv.org/abs/1906.07927>.
- [33] Anand Bhattad, Min Jin Chong, Kaizhao Liang, Bo Li, and David A. Forsyth. Big but Imperceptible Adversarial Perturbations via Semantic Manipulation. *arXiv:1904.06347 [cs]*, April 2019. URL <http://arxiv.org/abs/1904.06347>.
- [34] Sven Gowal, Chongli Qin, Po-Sen Huang, Taylan Cemgil, Krishnamurthy Dvijotham, Timothy A. Mann, and Pushmeet Kohli. Achieving robustness in the wild via adversarial mixing with disentangled representations. *CoRR*, abs/1912.03192, 2019. URL <http://arxiv.org/abs/1912.03192>.
- [35] Isaac Dunn, Hadrien Pouget, Tom Melham, and Daniel Kroening. Adaptive Generation of Unrestricted Adversarial Inputs. *CoRR*, abs/1905.02463, 2019. URL <http://arxiv.org/abs/1905.02463>.
- [36] Zhengli Zhao, Dheeru Dua, and Sameer Singh. Generating Natural Adversarial Examples. *arXiv:1710.11342 [cs]*, October 2017. URL <http://arxiv.org/abs/1710.11342>.
- [37] Yang Song, Rui Shu, Nate Kushman, and Stefano Ermon. Constructing Unrestricted Adversarial Examples with Generative Models. In Samy Bengio, Hanna M Wallach, Hugo Larochelle, Kristen Grauman, Nicolò Cesa-Bianchi, and Roman Garnett, editors, *Advances in Neural Information Processing Systems (NeurIPS)*, pages 8322–8333, 2018. URL <http://papers.nips.cc/paper/8052-constructing-unrestricted-adversarial-examples-with-generative-models>.
- [38] Shuo Wang, Shangyu Chen, Tianle Chen, Surya Nepal, Carsten Rudolph, and Marthie Grobler. Generating Semantic Adversarial Examples via Feature Manipulation. *arXiv:2001.02297 [cs, stat]*, January 2020. URL <http://arxiv.org/abs/2001.02297>.
- [39] Andrew Brock, Jeff Donahue, and Karen Simonyan. Large Scale GAN Training for High Fidelity Natural Image Synthesis. In *International Conference on Learning Representations (ICLR)*, 2019. URL <https://openreview.net/forum?id=B1xsqj09Fm>.
- [40] Mehdi Mirza and Simon Osindero. Conditional Generative Adversarial Nets. *CoRR*, abs/1411.1, 2014. URL <http://arxiv.org/abs/1411.1784>.
- [41] Nicholas Carlini and David A. Wagner. Towards evaluating the robustness of neural networks. In *2017 IEEE Symposium on Security and Privacy, SP 2017, San Jose, CA, USA, May 22-26, 2017*, pages 39–57. IEEE Computer Society, 2017. doi: 10.1109/SP.2017.49. URL <https://doi.org/10.1109/SP.2017.49>.
- [42] Olga Russakovsky, Jia Deng, Hao Su, Jonathan Krause, Sanjeev Satheesh, Sean Ma, Zhiheng Huang, Andrej Karpathy, Aditya Khosla, Michael S. Bernstein, Alexander C. Berg, and Fei-Fei Li. ImageNet Large Scale Visual Recognition Challenge. *International Journal of Computer Vision*, 115(3):211–252, 2015.
- [43] Kaiming He, Xiangyu Zhang, Shaoqing Ren, and Jian Sun. Deep residual learning for image recognition. In *2016 IEEE Conference on Computer Vision and Pattern Recognition, CVPR 2016, Las Vegas, NV, USA, June 27-30, 2016*, pages 770–778. IEEE Computer Society, 2016. doi: 10.1109/CVPR.2016.90. URL <https://doi.org/10.1109/CVPR.2016.90>.
- [44] Logan Engstrom, Andrew Ilyas, Shibani Santurkar, and Dimitris Tsipras. Robustness (Python library), 2019. URL <https://github.com/MadryLab/robustness>.
- [45] Eric Wong, Leslie Rice, and J. Zico Kolter. Fast is better than free: Revisiting adversarial training. In *8th International Conference on Learning Representations, ICLR 2020, Addis Ababa, Ethiopia, April 26-30, 2020*. OpenReview.net, 2020. URL <https://openreview.net/forum?id=BJx040EFvH>.

- [46] Yann LeCun, Corinna Cortes, and Chris Burges. MNIST Handwritten Digit Database. URL <http://yann.lecun.com/exdb/mnist/>.
- [47] Florian Tramèr, Jens Behrmann, Nicholas Carlini, Nicolas Papernot, and Jörn-Henrik Jacobsen. Fundamental tradeoffs between invariance and sensitivity to adversarial perturbations. *CoRR*, abs/2002.04599, 2020. URL <https://arxiv.org/abs/2002.04599>.
- [48] Daniel Kang, Yi Sun, Dan Hendrycks, Tom Brown, and Jacob Steinhardt. Testing Robustness Against Unforeseen Adversaries. *arXiv:1908.08016 [cs, stat]*, August 2019. URL <http://arxiv.org/abs/1908.08016>.
- [49] DeepMind. Biggan Deep 512l, 2019. URL <https://tfhub.dev/deepmind/biggan-deep-512l/1>.
- [50] Mingxing Tan and Quoc V. Le. Efficientnet: Rethinking model scaling for convolutional neural networks. In Kamalika Chaudhuri and Ruslan Salakhutdinov, editors, *Proceedings of the 36th International Conference on Machine Learning, ICML 2019, 9-15 June 2019, Long Beach, California, USA*, volume 97 of *Proceedings of Machine Learning Research*, pages 6105–6114. PMLR, 2019. URL <http://proceedings.mlr.press/v97/tan19a.html>.
- [51] Luke Melas-Kyriazi. lukemelas/EfficientNet-PyTorch, June 2020. URL <https://github.com/lukemelas/EfficientNet-PyTorch>. original-date: 2019-05-30T05:24:11Z.
- [52] Adam Paszke, Sam Gross, Francisco Massa, Adam Lerer, James Bradbury, Gregory Chanan, Trevor Killeen, Zeming Lin, Natalia Gimelshein, Luca Antiga, Alban Desmaison, Andreas Kopf, Edward Yang, Zachary DeVito, Martin Raison, Alykhan Tejani, Sasank Chilamkurthy, Benoit Steiner, Lu Fang, Junjie Bai, and Soumith Chintala. PyTorch: An imperative style, high-performance deep learning library. In H. Wallach, H. Larochelle, A. Beygelzimer, F. dAlché Buc, E. Fox, and R. Garnett, editors, *Advances in Neural Information Processing Systems 32*, pages 8024–8035. Curran Associates, Inc., 2019. URL <http://papers.neurips.cc/paper/9015-pytorch-an-imperative-style-high-performance-deep-learning-library.pdf>.
- [53] Diederik P. Kingma and Jimmy Ba. Adam: A Method for Stochastic Optimization. In Yoshua Bengio and Yann LeCun, editors, *3rd International Conference on Learning Representations, ICLR 2015, San Diego, CA, USA, May 7-9, 2015, Conference Track Proceedings*, 2015. URL <http://arxiv.org/abs/1412.6980>.
- [54] Alec Radford, Luke Metz, and Soumith Chintala. Unsupervised Representation Learning with Deep Convolutional Generative Adversarial Networks. In Yoshua Bengio and Yann LeCun, editors, *4th International Conference on Learning Representations, ICLR 2016, San Juan, Puerto Rico, May 2-4, 2016, Conference Track Proceedings*, 2016. URL <http://arxiv.org/abs/1511.06434>.
- [55] BorealisAI/advertorch, June 2020. URL <https://github.com/BorealisAI/advertorch>. original-date: 2018-11-29T22:17:33Z.

A Model details

A.1 BigGAN

We use the BigGAN-deep generator architecture at the 512×512 resolution, which can be found in Table 9 of Appendix B in the paper introducing BigGAN [39]. Conveniently, this table clearly indicates the locations at which we perturb the activations; every horizontal line of the table is a point at which our method can perturb the activation values. Please refer to Appendix B of the BigGAN paper for detailed descriptions, in particular of the ResBlocks which comprise the majority of the network. Note that we in essence perform perturbations after each ResBlock; if desired, perturbations could also be performed within each block. We take the pre-trained generator published by DeepMind [49].

A.2 Standard classifiers

We use two classifiers trained as usual to maximise accuracy on the training distribution. The first is from the state-of-the-art EfficientNet family [50], enhanced using noisy student training [2]. We use the best readily available model and pre-trained weights for Pytorch, EfficientNet-B4 (Noisy Student) from Melas-Kyriazi [51]. The second is PyTorch’s pre-trained ResNet50 [43], made available through the `torchvision` package of PyTorch [52]. These classifiers’ ImageNet accuracies are reported in Table 2.

Table 2: Classifiers’ accuracy on ImageNet, in %

Classifier	Top-1	Top-5
ResNet50	76.15	92.87
EfficientNet-B4 NS	85.16	97.47

A.3 Robust classifiers

We use two pre-trained ResNet50 classifiers adversarially trained against bounded pixel perturbations. The first, ‘ResNet50 Robust (Engstrom)’, from Engstrom et al. [44], was trained using l_2 -norm projected gradient descent attack with $\epsilon = 0.3$. The second, ‘ResNet50 Robust (“Fast”)’, from *Fast Is Better Than Free: Revisiting Adversarial Training* Wong et al. [45], was trained with the fast gradient sign method attack for robustness against l_∞ with $\epsilon = 4/255$. The classifiers’ ImageNet accuracies and robustness to relevant attacks are shown in Table 3.

Table 3: Classifiers’ accuracy on ImageNet, and robustness to attacks, in %

Classifier	Top-1 (no attack)	Top-1 (l_2 attack $\epsilon = 0.3$)	Top-1 (l_∞ attack $\epsilon = 4/255$)
ResNet50 Robust (Engstrom)	57.90	35.16	
ResNet50 Robust (“Fast”)	55.45		30.28

B Experimental setup

B.1 Technical details

For our experiments, we used the neural networks described in Appendix A, and searched for semantic perturbations using the procedure described in Sections 4 and 5. However, those sections did not describe the optimisation procedure used. We used the Adam optimiser [53] with a learning rate of 0.03 and the default β hyperparameters of 0.9 and 0.999. After each optimisation step, we constrained the magnitude of the perturbation by finding the L_2 norm of the perturbation ‘vector’ obtained by concatenating the scalars used to perturb each individual activation value, then rescaling it to have a norm no greater than our constraint. This constraint was initially set to be magnitude 1, and was slightly relaxed after each optimisation step by multiplication by 1.03 and addition of 0.1. These values were empirically found—using small amount of manual experimentation—to be a reasonable tradeoff

between starting small and increasing slowly enough to find decently small perturbations, while also using a reasonable amount of compute. Typically, finding a semantic perturbation under this regime takes $O(100)$ steps, which took $O(1)$ minute) using the single NVIDIA Tesla V100 GPU we used.

B.2 Data collection

We computed at least 240 examples to evaluate each classifier for each kind of perturbation; often many more. This used a fixed progression of randomly-sampled (y, z, t) tuples each time, where y is the desired true image label, z is the latent input to the generator, and t is the target label for the perturbed misclassification. This ensures direct comparability between classifiers and perturbation types, since the semantic perturbations are each time attempting to perturb the same unperturbed image $g(y; z)$ to be classified as label t .

As described in Section 5, we do not use the examples in our calculations if the classifier misclassifies the unperturbed image, or if a human judges that the correct label is not the desired label y . We also filter out those perturbed images for which y does not remain the true label, although Figure 5 also shows the results with these included as dotted lines. To elicit a judgement about whether a particular image is indeed of label y , we ask a human participant which of the following four options is the best description of the image:

1. “This is an image of label y ”
2. “This is an image of something else”
3. “It is unclear what this image shows”
4. “This is not an image of anything meaningful”

We use the clear interface shown in Figure 6 to collect these data, and use the measures described in Section 5.3 to minimise threats to validity.

C ImageNet: further examples

We include a number of examples here, for convenient perusal, but these are limited by space and file size constraints. Therefore, we also provide *all* examples and raw results from our experiments as an anonymous download, to allow the reader to view the full range of perturbation types and validate that the results are reasonable. Here is the link: <https://doi.org/10.5281/zenodo.3889777>.

C.1 Effect of layer perturbed and classifier evaluated

Figures 7 to 10 further illustrate the effect of performing semantic perturbations to different sets of neurons in the generator, while evaluating different kinds of classifier. The initial (y, z, t) tuples selected are chosen so that all sixteen perturbed images for each were judged not to have changed class. These examples again show the range of feature granularities affected by perturbing activations at different stages in the generator. They also show visually that, in contrast to the adversarially-trained classifiers, the classifiers which underwent standard training need only small perturbations to fine-grained features but require large perturbations to their high-level features to induce the targeted misclassification.

C.2 Various examples

Figures 12 and 11 show the results for perturbing the first sixteen randomly-selected (y, z, t) tuples.

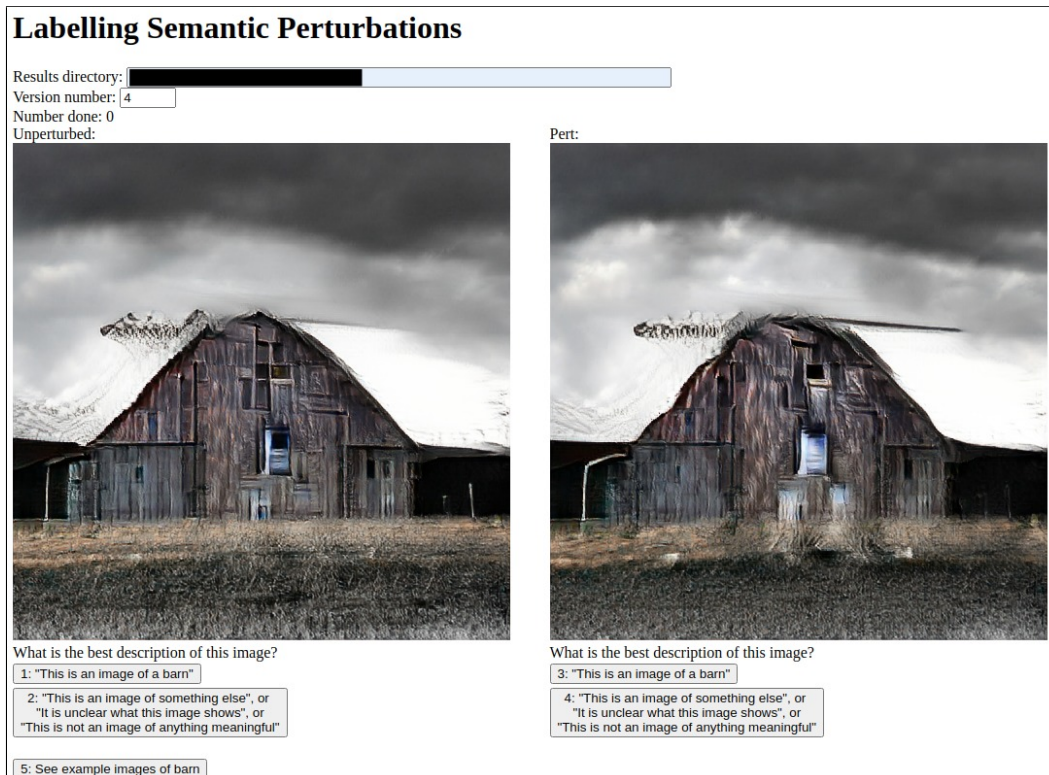


Figure 6: Screenshot of labelling interface. The perturbed image and buttons, on the right-hand side, are visible only when the unperturbed image (on the left) has been selected as matching the desired label. The buttons are numbered to provide keyboard shortcuts. The button at the bottom opens a web image search, in case the user is unfamiliar with the class label.

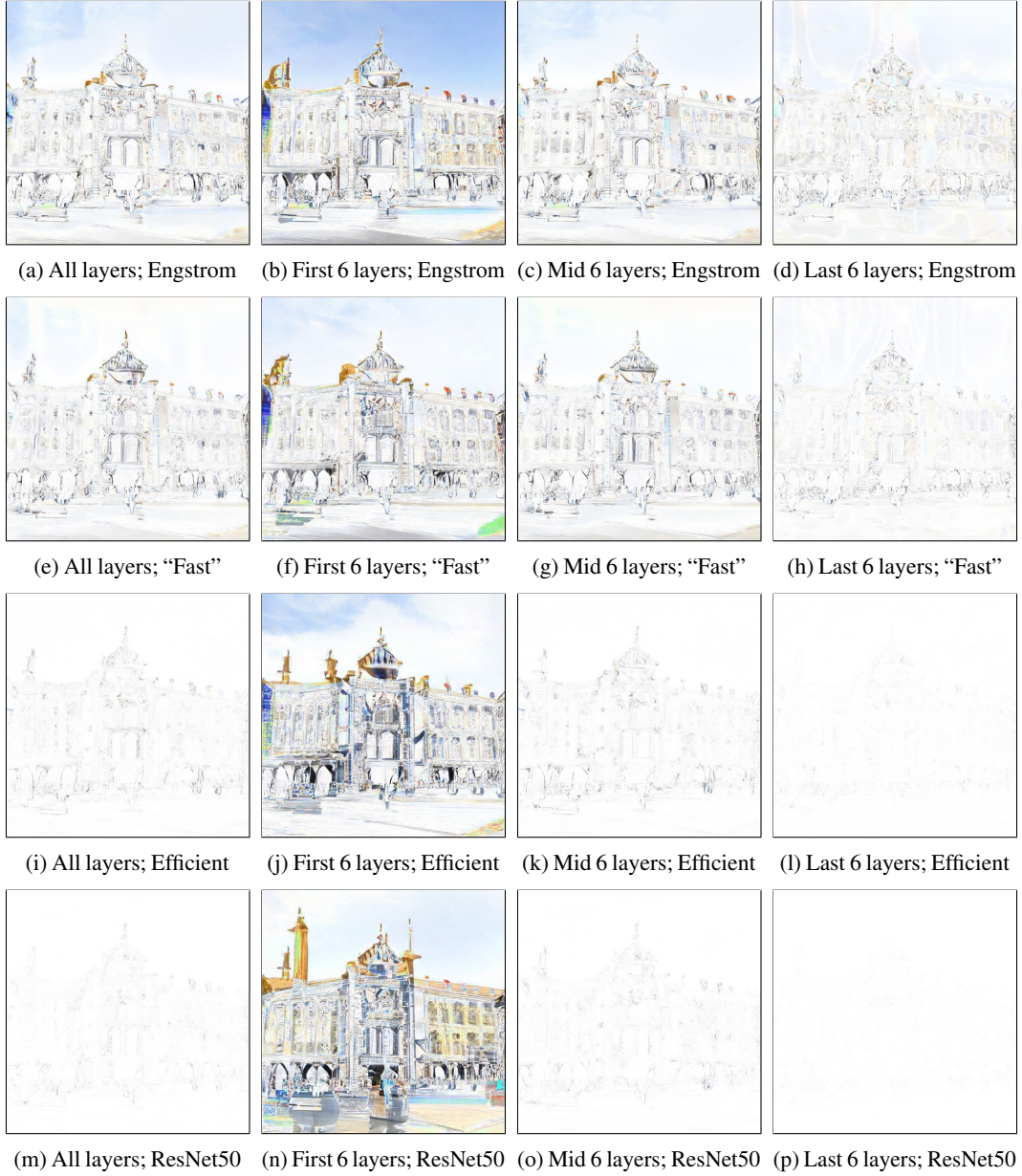


Figure 7: Demonstration of the effect of semantic perturbations performed when restricted to the activations in only certain layers; each column allows a different subset of activations to be perturbed. Results are shown for four classifiers, with one classifier per row: two adversarially-trained classifiers (Engstrom et al. [44] and "Fast" [45]), EfficientNet-B4 NS [2], and standard ResNet50 [43]. Note how the granularity of features perturbed varies with perturbations to different activations. Note also how the non-robust classifiers (bottom two rows) require a relatively large perturbation in the first six layers.



Figure 8: The perturbed images corresponding to Figure 7. Note the range of semantic features perturbed, varying from changing the weather (b and j) and the architecture (n) to increasing the visibility and brightness of flags (c) to minute changes to the position of low-level edges.



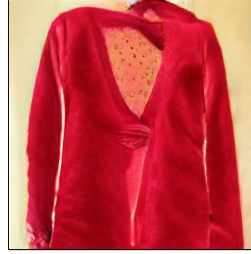
Figure 9: Replication of Figure 7 with another example image.



Figure 10: The perturbed images corresponding to Figure 9.



(a) Skipped because the classifier did not predict the desired label, 'Labrador retriever'.



(b) Skipped because the human did not agree that 'velvet' was the best description of the unperturbed image.



(c) Perturbed from 'Komodo dragon' (left) to 'overskirt' (right), but the human labeller did not agree that the label 'Komodo dragon' remained the best description of the perturbed image.



(d) Perturbed from 'file cabinet' (left) to 'doormat' (right); the human judged the true label of the perturbed image to remain unchanged.



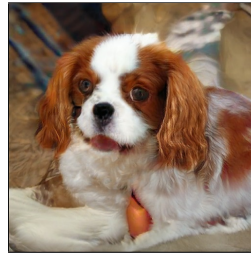
(e) Perturbed from 'barn' to 'Afghan hound'; the human judged the true label of the perturbed image to remain unchanged.



(f) Perturbed from 'palace' to 'throne'; the human judged the true label of the perturbed image to remain unchanged.

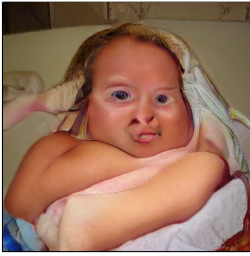


(g) Perturbed from 'reflex camera' to 'sunglass'; the human judged the true label of the perturbed image to remain unchanged.

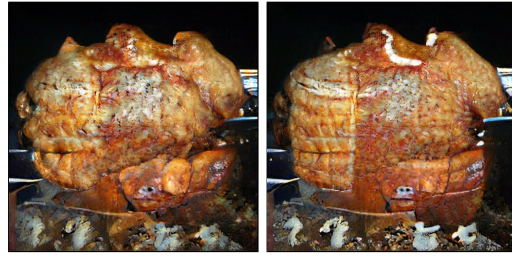


(h) Perturbed from 'Blenheim spaniel' to 'black-and-tan coonhound'; the human judged the true label of the perturbed image to remain unchanged.

Figure 11: The first examples used in our experiments, continued. Engstrom et al.'s adversarially-trained classifier [44] is the classifier being evaluated. Captions indicate whether each example was skipped, or the label judgements. Perturbed images are to the right of each unperturbed image.



(a) Skipped because the classifier did not predict the desired label, 'bath towel'.



(b) Perturbed from 'rotisserie' to 'rain barrel'; the human judged the true label of the perturbed image to remain unchanged.



(c) Perturbed from 'breastplate' to 'mud turtle'; the human judged the true label of the perturbed image to remain unchanged.



(d) Skipped because the human did not agree that 'spotted salamander' was the best description of the unperturbed image.



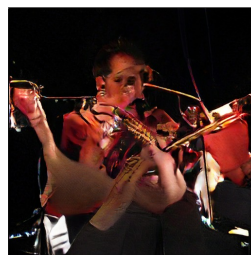
(e) Perturbed from 'yurt' to 'library'; the human judged the true label of the perturbed image to remain unchanged.



(f) Perturbed from 'cougar' to 'shower cap'; the human judged the true label of the perturbed image to remain unchanged.



(g) Perturbed from 'chickadee' to 'soap dispenser'; the human judged the true label of the perturbed image to remain unchanged.



(h) Skipped because the classifier did not predict the desired label, 'trombone'.

Figure 12: The first examples used in our experiments, with randomly-selected source and target labels. Engstrom et al.'s adversarially-trained classifier [44] is the classifier being evaluated. Captions indicate whether each example was skipped, or the label judgements.

Table 4: MNIST convolutional generator architecture. Each new line represents a new layer. Each horizontal lines marks an activation tensor at which semantic perturbations are performed.

Fully-Connected	(64 units)
ReLU	
Transposed Convolution	(5×5 kernel, 2×2 stride, 32 feature maps)
Batch Normalisation	
Leaky ReLU	(Slope -0.2)
Dropout	($p=0.35$)
Transposed Convolution	(5×5 kernel, 2×2 stride, 8 feature maps)
Batch Normalisation	
Leaky ReLU	(Slope -0.2)
Dropout	($p=0.35$)
Transposed Convolution	(5×5 kernel, 2×2 stride, 4 feature maps)
Batch Normalisation	
Leaky ReLU	(Slope -0.2)
Dropout	($p=0.35$)
Fully-Connected	(784 units)
Sigmoid	(tanh used during training)

D MNIST

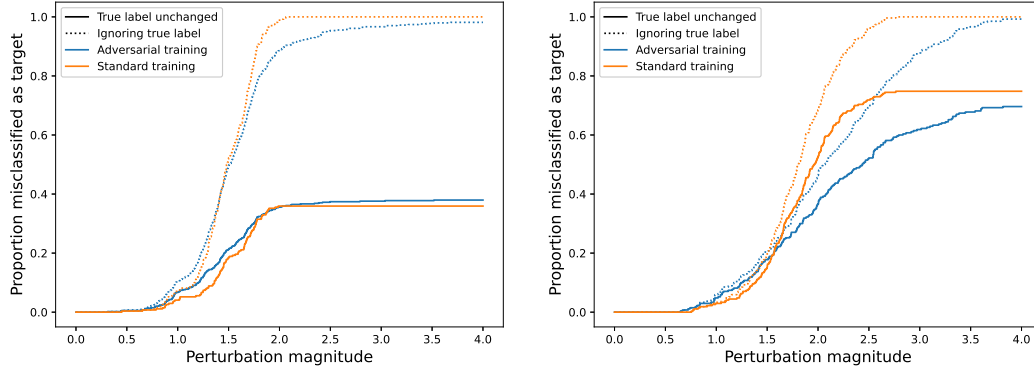
D.1 Model details

MNIST convolutional GAN For MNIST, we tried a range of generators and found that they all worked roughly as well as one another. For the experiments, we use a simple convolutional generator, inspired by the Deep Convolutional GAN [54]. Details are shown in Table 4. Inputs to the generator are drawn from a 128-dimensional standard Gaussian. The sigmoid output transformation ensures that pixels are in the range $[0, 1]$, as expected by the classifiers. We perform semantic perturbations before ReLU layers, rather than after, to prevent ReLU output values from being perturbed to become negative, which would not have been encountered during training and so may not result in plausible images being generated since they are out-of-distribution for the rest of the generator. Note that perturbing before and after the sigmoid transformation has different effects because perturbations to values not close to 0 are diminished in magnitude if passed through the sigmoid function.

Classifiers We use two neural networks that classify MNIST. One is a simple standard classifier with two convolutional layers and three fully-connected layers, trained to give an accuracy over 99%. The other is an LeNet5 classifier adversarially trained against l_2 -norm bounded perturbations for $\epsilon = 0.3$. This was trained using the AdverTorch library [55]. It has a standard accuracy of 98%, reduced to 95% by an l_2 -norm bounded attack with $\epsilon = 0.3$.

D.2 Experimental setup

We find semantic perturbations as described for ImageNet in Appendix B, with a few differences. First, since the generator is much smaller, we divide it nearly in half, comparing the effect of perturbing



(a) Generator activations perturbed at first 4 layers only. (b) Generator activations perturbed at last 4 layers only.

Figure 13: Graphs showing how the proportion of perturbations that induce the targeted misclassification increases with perturbation magnitude. These should be interpreted as Figure 5. The solid lines exclude the perturbed images for which a human judges that the perturbation does not change the true label of the image; the dotted lines, for reference, include these.

the activation values at first four layers only with the effect of perturbing at the last four layers only. Second, because MNIST (and the generator) is much smaller, so are the perturbation magnitudes required. So the learning rate is reduced to 0.004, the we start with an initial perturbation magnitude constraint of 0.1, and this is gradually relaxed after each optimisation step by increasing this upper bound by 0.001. The procedure for collecting human judgements is as described in Appendix B.

D.3 Results and discussion

Figure 13 shows the robustness of the two classifiers to the two kinds of semantic perturbation. We can see from Figure 13b that the classifier trained to be robust to pixel-space perturbations is indeed more robust than the standard classifier, with its considerably shallower slope indicating that a bigger perturbation magnitude is required to the finer-grained features encoded in the last four layers of the generator.

Conversely, Figure 13a gives an almost-identical shape for both classifiers, indicating that adversarial training against pixel-space perturbations does not confer any robustness to the coarse-grained semantic perturbations being evaluated here. This has an interesting relationship with our main finding, that adversarial training against pixel-space perturbations seriously harms robustness to high-level semantic features perturbations on ImageNet. The difference can likely be best explained by the great difference in datasets. The dimensionality of ImageNet is over $1000\times$ greater, and the high-level semantic feature space of MNIST is trivially small in comparison. The result of this is that in some loose sense, there is a smaller ‘gap’ between the highest- and lowest-granularity features encoded in the generator; put another way, there is a much less rich space of coarse-grained semantic features that a classifier must be robust to on MNIST.

Whether this is the correct intuition, the implications of our finding remains clear: even on the very simplest datasets, robustness to fine-grained features completely fails to generalise to more semantic features. If we are to obtain classifiers that we can trust to generalise under modest distributional shifts, there is still far to go.



Figure 14: Random sample of semantic perturbations targeting label 0. Only the first four layers of generator activations are perturbed, and the classifier is trained using a standard training procedure. In each pair, the perturbed image is to the right of the unperturbed image.

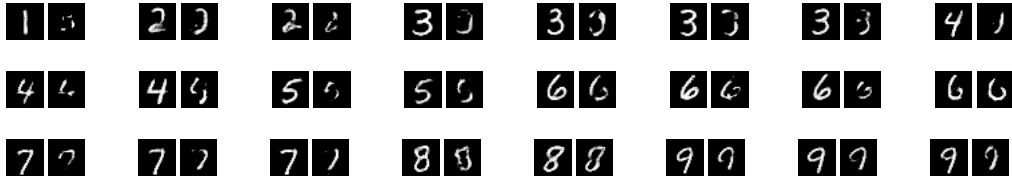
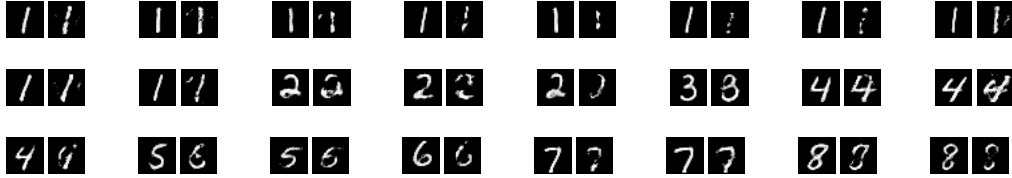


Figure 15: Random sample of semantic perturbations targeting label 0. Only the first four layers of generator activations are perturbed, and the classifier is trained using adversarial training. In each pair, the perturbed image is to the right of the unperturbed image.



Random sample of semantic perturbations targeting label 0. Only the last four layers of generator activations are perturbed, and the classifier is trained using a standard training procedure. In each pair, the perturbed image is to the right of the unperturbed image.

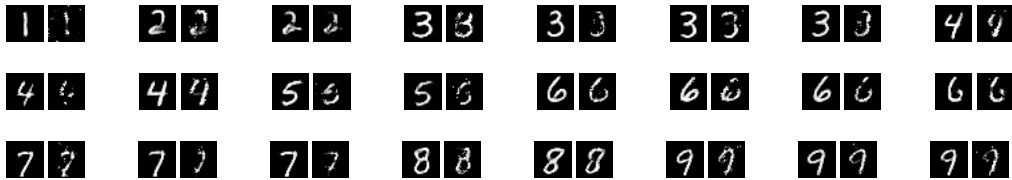


Figure 16: Random sample of semantic perturbations targeting label 0. Only the last four layers of generator activations are perturbed, and the classifier is trained using adversarial training. In each pair, the perturbed image is to the right of the unperturbed image.